SPHEROMAK TILTING AND ITS STABILITY CONTROL

T.Hayashi and T.Sato

Institute for Fusion Theory, Hiroshima University
Hiroshima 730, Japan

1. Introduction

Its innovative concept as a fusion reactor, notwithstanding, spheromak configuration is globally unstable, particularly tilt unstable. The tilt instability is already experimentally[1] and numerically[2] observed. Stability analysis[3] states that a conducting wall close to a spheromak plasma could stabilize the instability. Experimentally, it is also confirmed that a figure eight or a saddle coil acts to stabilize it, though eventually it suffers a tilting instability[1].

The purpose of this presentation is three-hold. First, we attempt to invent a numerical technique to create a rather arbitrarily-shaped spheromak like the one with a flux hole. Secondly, we study extensively the dynamics governing the tilting instability, namely, the influence of the magnetic index, the toroidal current (q-profile) and the resistivity upon the tilting growth rate, and the roles of magnetic reconnection upon the nonlinear development. The third purpose is an attempt to invent the best way to control the tilting instability. We have tried to clarify stabilizing effects of the distance of the horizontal and vertical walls and the radius of the center poles. We also studied the influence of the wall condition, namely, whether the wall acted as a flux conserver in the spheromak creation stage or not.

2. Creation of a spheromak with a flux hole

In order to create a spheromak numerically we adopted the Princeton slow induction scheme[2]. In our numerical scheme that employs the two-step Lax-Wendroff method, a smoothing procedure is needed to insure a numerical instability. For this purpose we make a four-point average over the 25% of the difference value ($f - f_0$) at every n time steps where f is each

variable and f_0 is a reference value which is updated by its own value at every m time steps ($m > n$). By properly choosing n and m we can optimize the numerical stability and the induced spheromak current.

In the operation of spheromak creation we have two time scales T_{sp} and T_{st} where T_{sp} is the operation time of poloidal flux control and T_{st} is the time controlling the toroidal flux. When $T_{sp} < T_{st}$, no flux hole is created but a classical type spheromak is created. When T_{st}/T_{sp} decreases, on the other hand, a larger flux hole is formed. A typical spheromak with a flux hole thus created is shown in Fig. 1.

3. Dynamics of tilting instability

In Fig. 2 we present a typical tilting behavior. The upper frame shows the tilt angle versus time. Corresponding spheromak forms are shown in the lower frame which are viewed from two azimuthal angles perpendicular to each other. We observe two remarkable facts. One is the fact that as the spheromak tilts substantially, an asymmetry appears, namely, that one side of the torus is eroded and disappears when it tilts roughly 90°. We note later on that this is due to magnetic reconnection. Another remarkable fact is that after this reconnection (erosion) phase a helically-skewed cylindrical blob continues to survive sufficiently long time, and decays, presumably, by diffusion. This indicates that the complicated helically-skewed structure is magnetohydrodynamically stable. In other words, the tilted spheromak appears to relax toward a different minimum energy state. Color movie (in the presentation) that traces the evolution of magnetic field lines clearly indicates a partial realization of field-reversal configuration.

In the above we have seen that spheromak tilts and the tilting spheromak suffers reconnection which plays a vital role in the spheromak life[2]. In the following we summarize the relationships between the tilting growth and several controlling parameters.

Fig. 3 shows a comparison between two cases with different toroidal current distributions. It is evident that a spheromak having a sharply peaked current tilts much more rapidly.

Fig. 4 shows tilting developments for different magnetic indices, which indicates a clear dependence of the tilt speed on the magnetic index.

In the next, we shall describe the influence of the resistivity upon the tilting dynamics. The magnetic Reynolds number S is changed from 54 to infinity (S does not include numerical diffusion). Simulation runs have shown that the spheromak evolution can be characterized by three categories. For S < 1000, diffusion is a dominant process and spheromak shrinks rather quickly, so that no tilting occurs. For S > 5000, on the other hand, spheromak suffers a tilting instability and is eroded by reconnection. In the intermediate S region, both shrinking by diffusion and tilting by toroidal current take place simultaneously.

Shown in Fig. 5 are the tilt angles for S = 54,000 and S = 5,400. The tilt behavior is similar to each other. However, the disruption speed for S = 5,400 is faster than that for S = 54,000. This difference may be ascribed to the reconnection speed. To visualize this difference, we show a time series of snapshots of a toroidal field contour surface in Fig. 6.

4. Stability control

In this section we do a parameter search for finding a useful way of supressing the dangerous tilting instability. In the first place, we examine the wall stabilization.

4.1 Wall stabilization

Three different cases are studied, namely, the vertical wall, isolated conducting cylindrical belt, and horizontal wall. In order to study these effects, we first create a nearly equilibrium spheromak in a usual way and then place a wall in a certain position. By running a code with new boundary conditions, we examine the wall stabilization effect.

4.1.1 Vertical wall

In the first run the wall is placed at $r_w = 0.75$m (the vacuum vessel is a cylinder with r = 1.5m and z = ±0.75m). In this case tilt speed is somewhat slowed down compared with the case with no wall. When the wall position is changed to $r_w = 0.67$m, the speed is further decreased, but the decrease is rather small (see Fig.7). When we moved the wall a bit nearer to the spheromak, namely, $r_w = 0.625$, surprisingly tilt is completely supressed as if it is tied to the wall. It turns out that this dramatic change ocurred at $r_w = 1.4r_s$ where r_s stands for a rough spheromak radius. Thus, we can conclude that a vertical wall can stop the

tilting instability if the wall is approximately within $1.4r_s$, this being consistent with Jardin et al[3].

4.1.2 Cylindrical ring

To know whether or not the above stabilization can be achieved by a partial wall which does not engulf the spheromak, we have provided three partial rings at r = 0.583m, the radial width being 0.08m and the vertical height being 0.33, 0.67 and 1.33m. Tilt angles as a function of time are shown in Fig. 8 for three cases. This indicates that the tilt tends to be stabilized as the height of the ring increases. Importantly, however, no complete suppression can be realized by a partial wall even though the height is very close to the wall of the vacuum vessel.

4.1.3 Horizontal wall

Similarly to the case with the vertical wall, we put a horizontal wall at $z_w = \pm 0.42$m. Tilting evolution is slowed down as can be seen in Fig. 9. When the wall distance is reduced to $z_w = \pm 0.33$m, tilting is again completely supressed. In this case roughly $z_w = 1.3z_s$ where z_s is the spheromak radius in the z direction. Thus, we can conclude that not only the vertical wall, but also the horizontal wall can supress the tilting instability as far as the distance from the spheromak is within a certain distance, which is in contrast with Jardin et al[3].

4.1.4 Vacuum vessel

We also have examined how the vacuum vessel wall can contribute to stabilization. For this purpose we have made simulations with the same operational mode where the vertical dimension of the vacuum vessel is changed from the initial stage. In this case, therefore, the total flux is conserved. Three runs are made for z = ±0.42m, 0.33m and 0.25m. Tilt angles are shown in Fig.10. Obviously, there is a marked difference in the time when tilt appears appreciable. As the vessel dimension is smaller, the tilt starts later. However, the nonlinear growth appears larger for smaller dimensions, presumably because the spheromak size is smaller. Here we note that in the last case tilt direction was opposite to the applied perturbation. This may be interpreted as a result of nonlinear up and down bouncing motion arising from the fast Alfven bounce motion.

4.2 Central pole stabilization

We have run four cases where the radius of the center pole is

r_p = 0.08m, 0.17m, 0.25m and 0.33m. In these runs the pole was assumed to exist from the initial condition. Tilt angle versus time is again plotted for all cases in Fig. 1?. As can be seen from this figure, spheromak tends to be stabilized as the pole radius increases. When r_p = 0.25m, it tilts but the tilt stops at a certain angle and stays in its position for a rather long time. When r_p = 0.33m, tilt is supressed, however, the spheromak shape is smashed on the pole side.

5. Conclusion

The present study has shown that the 3-D simulation is indeed useful and practical in not only studying the underlying physics but also finding a stabilization technique of spheromaks.

References

1. Private communication with Drs. M.Yamada and A.Janos
2. T.Sato and T.Hayashi, Phys.Rev.Lett. 50, 38 (1983).
3. S.C.Jardin et al., Nuclear Fusion, 21, 1203 (1981).

Figure Captions

Fig.1 Cross sectional view of several quantities of a typical spheromak with flux hole

Fig.2 Typical tilting behaviors

Fig.3 Tilt angle versus time for different toroidal currents

Fig.4 Tilt angle versus time for different magnetic indices

Fig.5 Tilt angle versus time for different magnetic Reynolds number

Fig.6 Typical example showing the tilting deformation (plotted are the contour surfaces of toroidal field component)

Fig.7 Tilt angle versus time for different vertical wall positions

Fig.8 Tilt angle versus time for different cylindrical rings

Fig.9 Tilt angle versus time for different horizontal wall positions

Fig.10 Tilt angle versus time for different vacuum vessel sizes

Fig.11 Tilt angle versus time for different central pole sizes

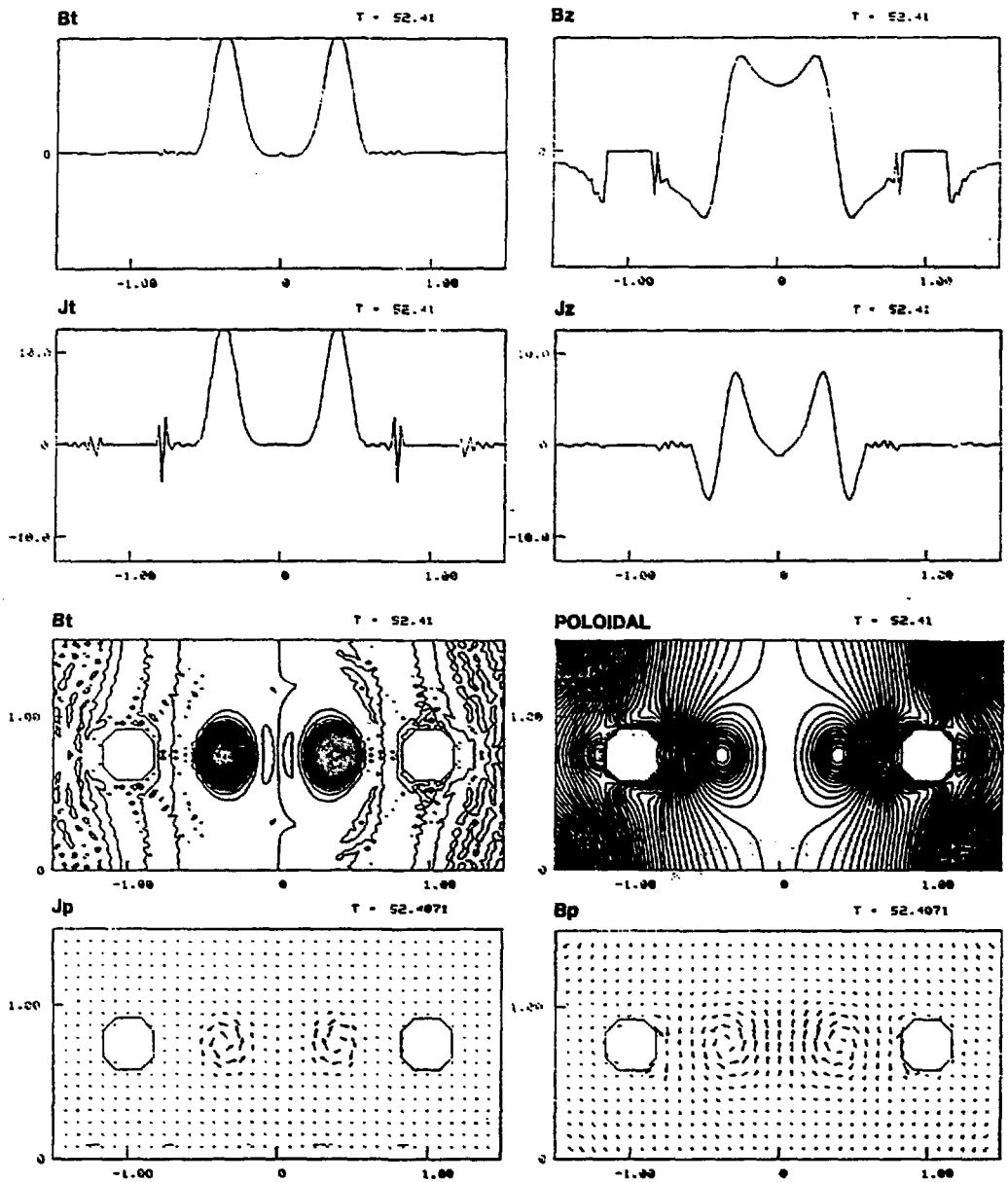
Bt
T = 52.41
Bz
T = 52.41
Jt
T = 52.41
Jz
T = 52.41
Bt
T = 52.41
POLOIDAL
T = 52.41
Jp
T = 52.4071
Bp
T = 52.4071

Fig. 1

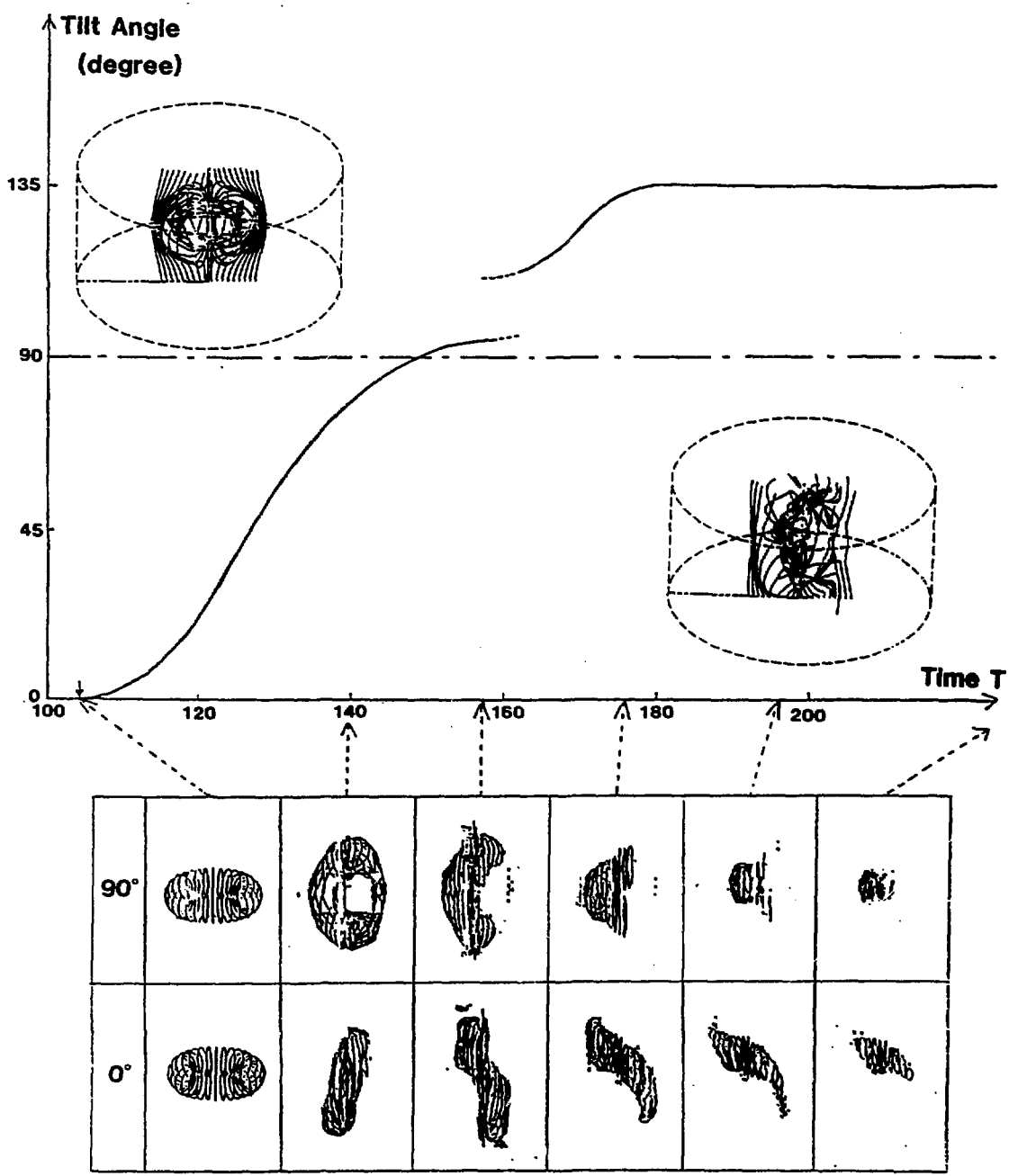

Fig.2

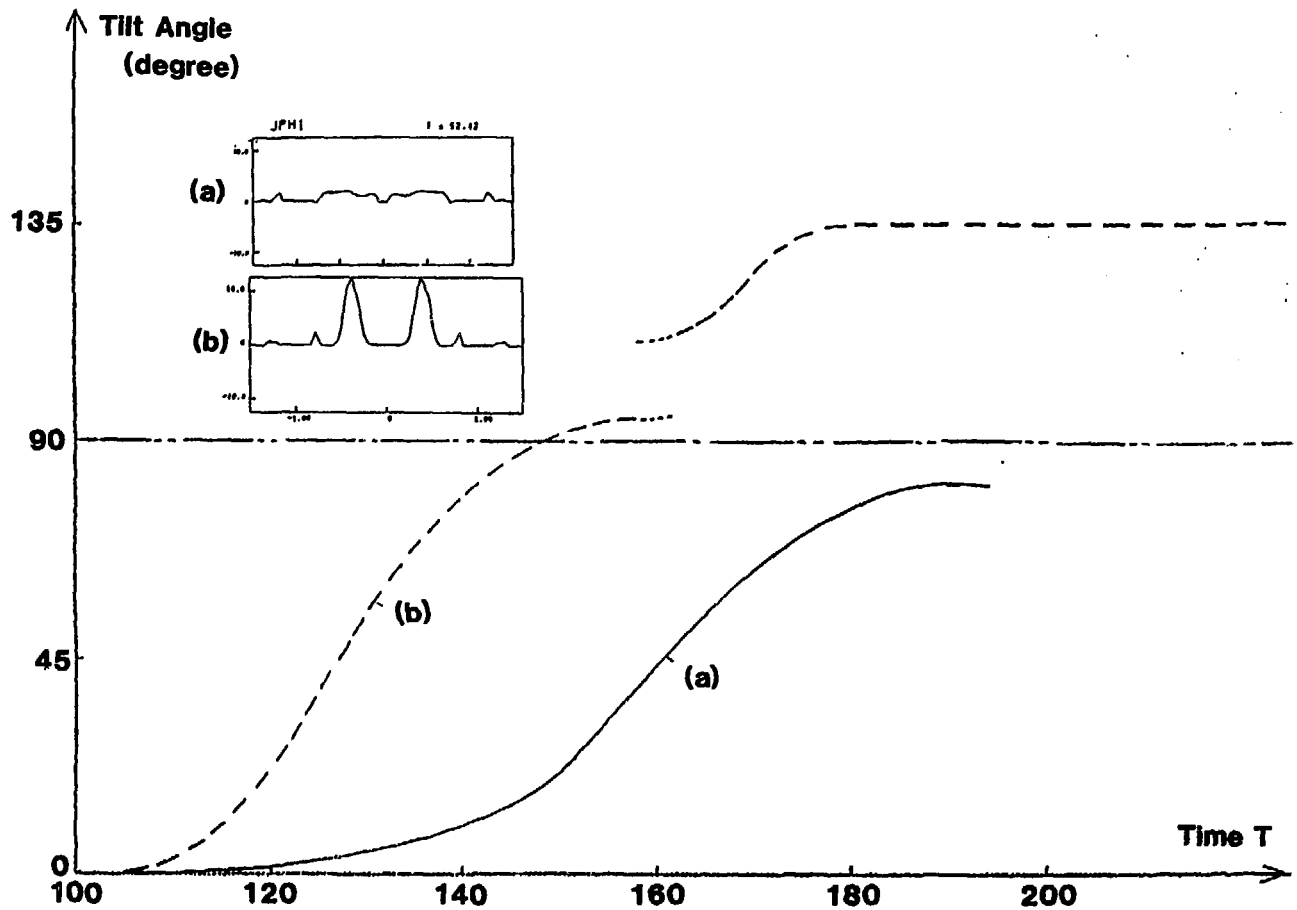
Tilt Angle
(degree)
135
90
45
0
100
120
140
160
180
200
Time T
(a)
(b)
(a)
(b)

Fig.3

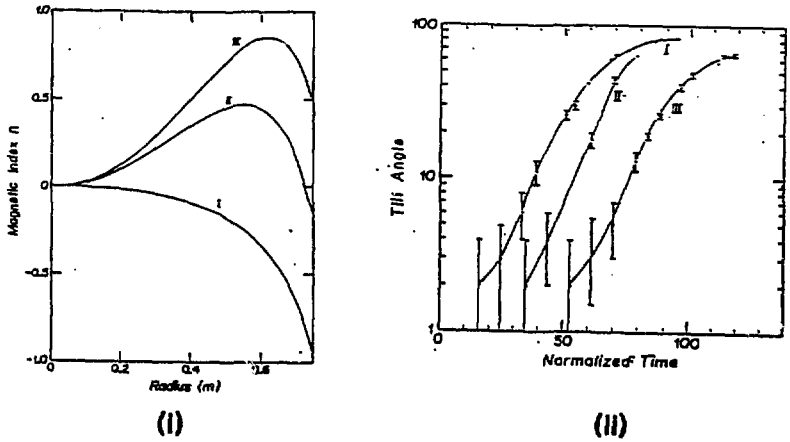

(I) (II)

Fig.4

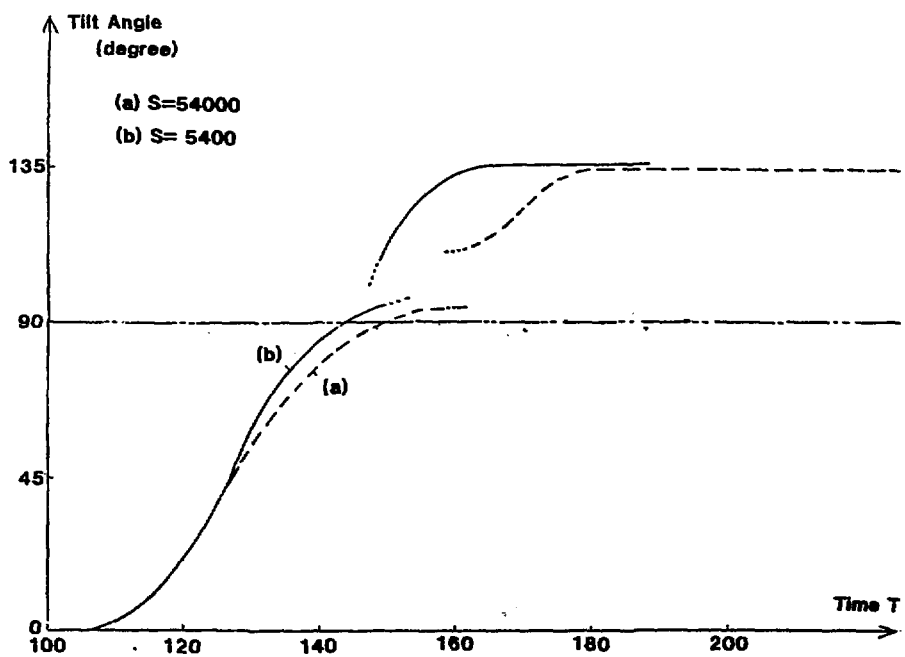

Fig.5

T \ S	S=54000	S= 5400
104.8		
113.6		
122.3		
131.1		
139.9		
148.6		

T \ S	S=54000	S= 5400
157.4		
166.2		
174.9		
196.8		
231.9		
275.7		

Fig.6

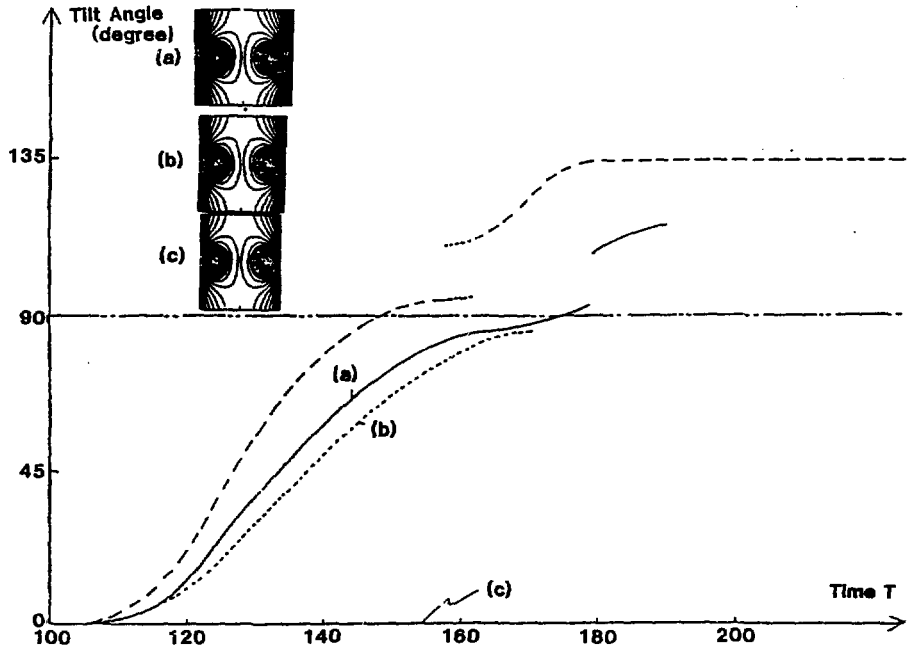
Tilt Angle
(degree)
(a)
(b)
(c)
135
90
45
0
(a)
(b)
(c)
Time T
100
120
140
160
180
200

Fig.7

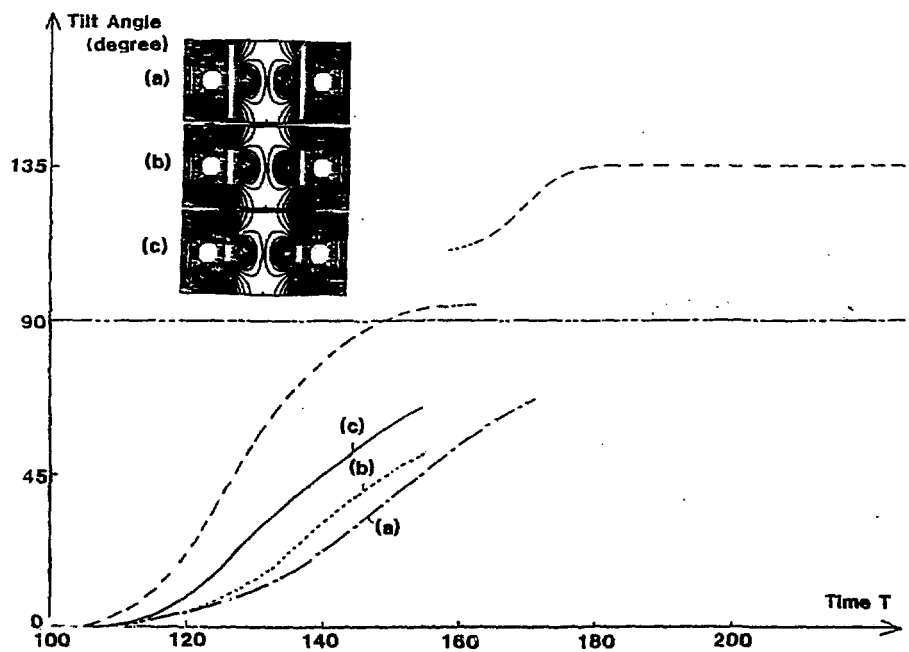
Tilt Angle
(degree)
(a)
(b)
(c)
135
90
45
0
(c)
(b)
(a)
Time T
100
120
140
160
180
200

Fig.8

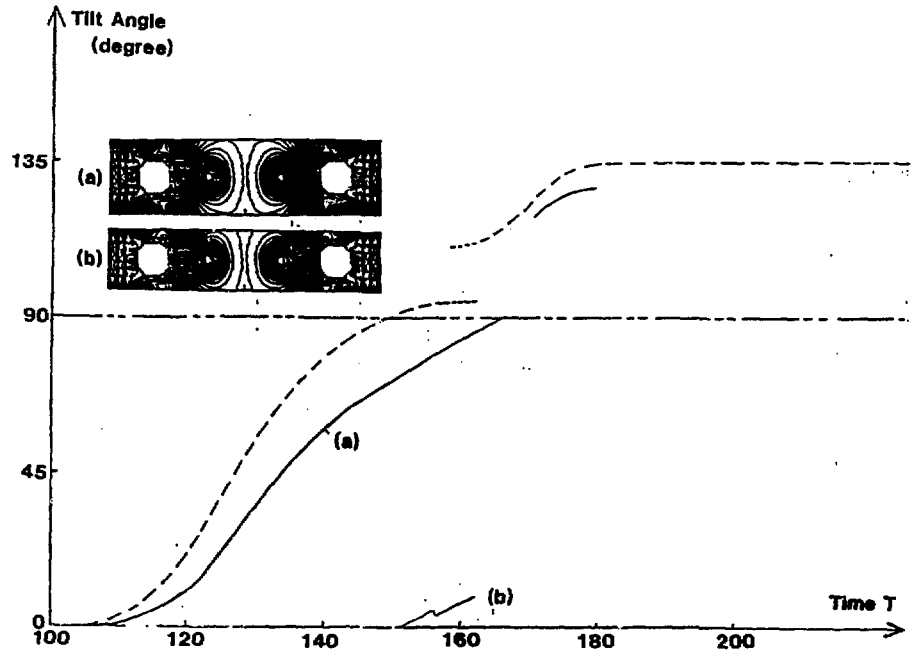
Tilt Angle
(degree)
135
90
45
0
(a)
(b)
(a)
(b)
100
120
140
160
180
200
Time T

Fig.9

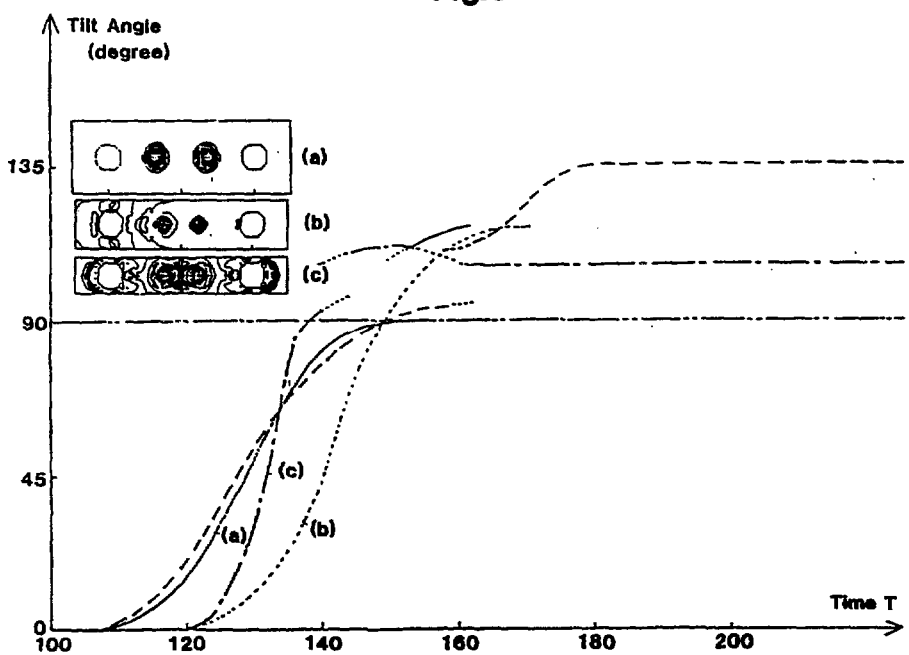
Tilt Angle
(degree)
135
90
45
0
(a)
(b)
(c)
(c)
(a)
(b)
100
120
140
160
180
200
Time T

Fig.10

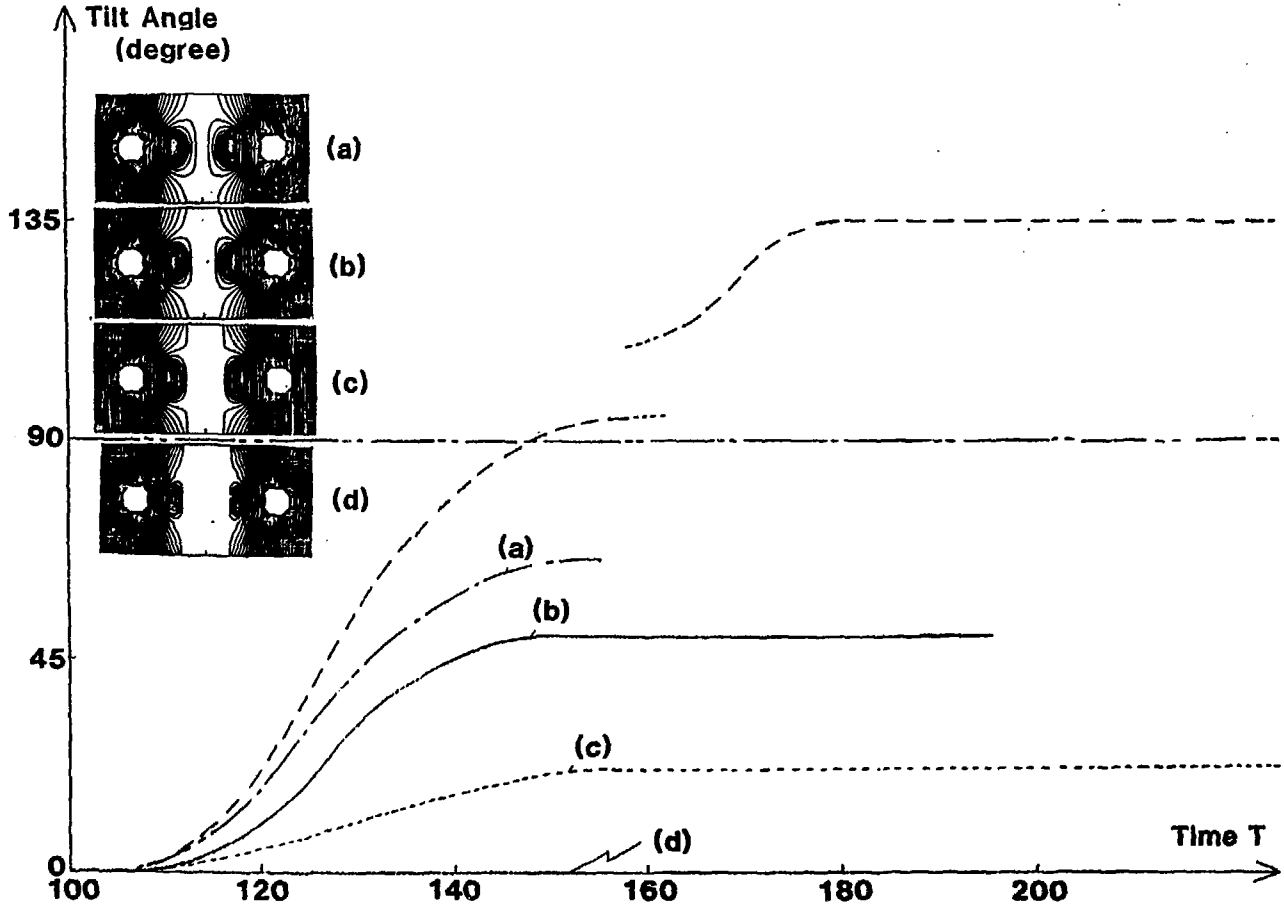
Tilt Angle
(degree)
135
90
45
0
(a)
(b)
(c)
(d)
(a)
(b)
(c)
(d)
Time T
100
120
140
160
180
200

Fig.11